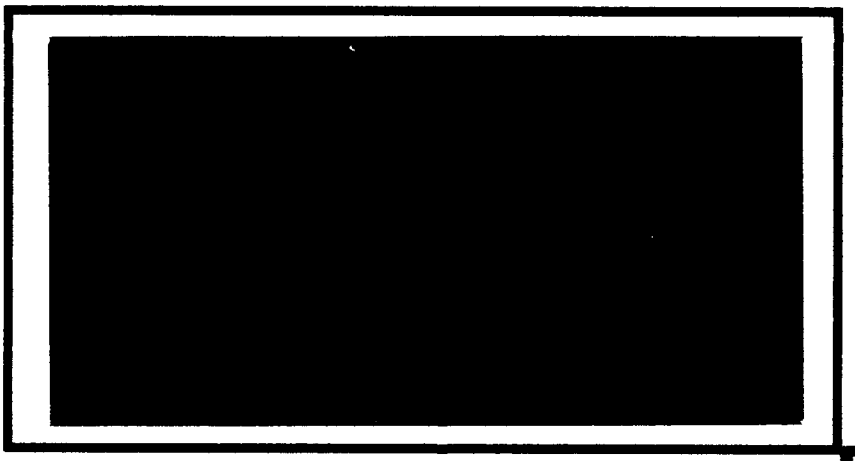

DEPARTMENT OF THE AIR FORCE

AIR UNIVERSITY

AIR FORCE INSTITUTE OF TECHNOLOGY

Wright-Patterson Air Force Base, Ohio

AFIT/GA/ENY/90D-02

ANALYSIS OF PARKING ORBITS FOR A STS EXTERNAL TANK IN LOW EARTH ORBIT

THESIS

James E. Cross, Captain, USAF

AFIT/GA/ENY/90D-02

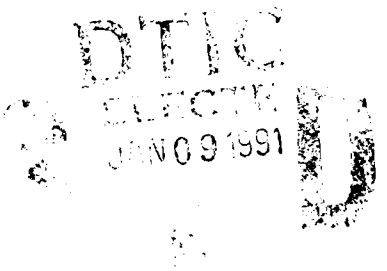

AFIT/GA/ENY/90D-02

ANALYSIS OF PARKING ORBITS FOR A STS EXTERNAL TANK IN LOW EARTH ORBIT

THESIS

Presented to the Faculty of the School of Engineering
of the Air Force Institute of Technology
Air University
In Partial Fulfillment of the
Requirements for the Degree of
Master of Science in Astronautical Engineering

James E. Cross, B.S.
Captain, USAF

December 1990

Preface

The purpose of this study was to analysis the orbital dynamics of a space shuttle external tank taken into low Earth orbit. This was not a feasibility study, however the results obtained from this research would be very useful to someone contemplating the viability of using external tanks on orbit. In performing the research and writing this thesis I have had a great deal of help from others. I am deeply indebted to my faculty advisor, Capt Rodney D. Bain. I also wish to thank my classmates for their support and encouragement, without which I would not have been able to complete this study.

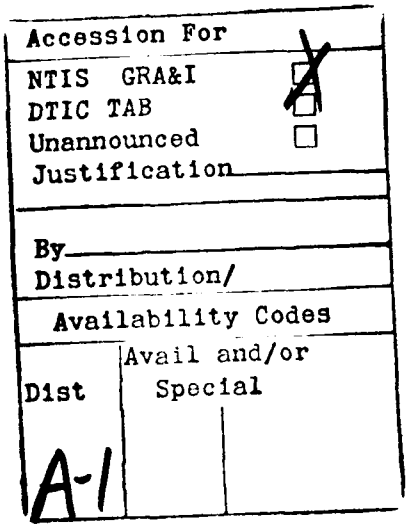

Table of Contents

List of Figures

I THE PROBLEM

One of the main goals of the Space Transportation System (STS) is to reduce the cost of delivering payloads into orbit. Reuse of the solid rocket boosters and orbiter itself is a major factor in achieving this goal, but the original Space Shuttle designers elected to make the external tank (ET) an expendable element of the STS. A typical launch will retain the ET for the space shuttle main engine (SSME) burn of over eight minutes and then jettison it for a controlled entry into the Indian or Pacific Ocean. However, this component of the STS does not have to go to waste. When cast off, the external tank has 98% of the energy needed to insert it into orbit. A launch trajectory, called the direct injection, could be flown whereby the space shuttle main engines would boost the orbiter with its attached external tank into a standard shuttle orbit. See Figure 1. The use of this more efficient flight path would not only allow the tank to be taken into orbit, but an additional 2000 lbs of payload could be carried. The orbiter would then leave the ET and continue on its scheduled mission. In other words, its costs nothing to deliver a 53,000 lb, factory tested, aluminium pressure vessel into low Earth orbit (8:I-1).

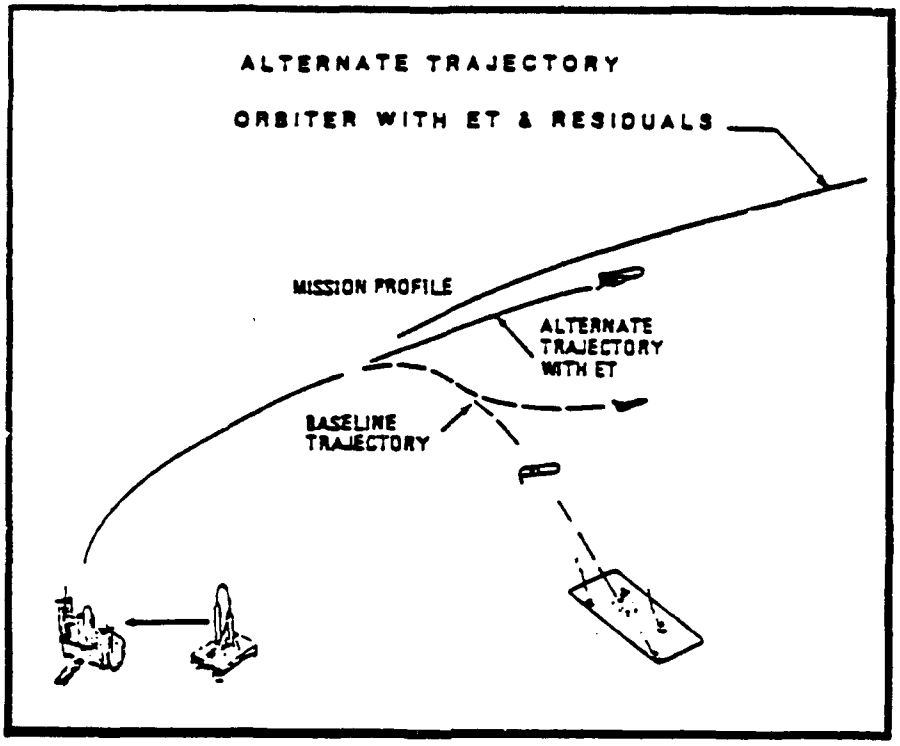

Fig. 1 Direct Insertion Launch Trajectory

The external tank is the main structural element of the STS, supporting both the orbiter and the two solid rocket boosters. The tank consists of three main components: the liquid oxygen tank, the intertank, and the liquid hydrogen tank. See Figure 2. These ET components are manufactured from an aluminum alloy, and after assembly the unit is coated with a 1 to 1-1/2 inch layer of spray on foam insulation (8:II-1).

Taking the ET into orbit presents several opportunities and capabilities. Reference 8 describes many on-orbit applications for an ET which have

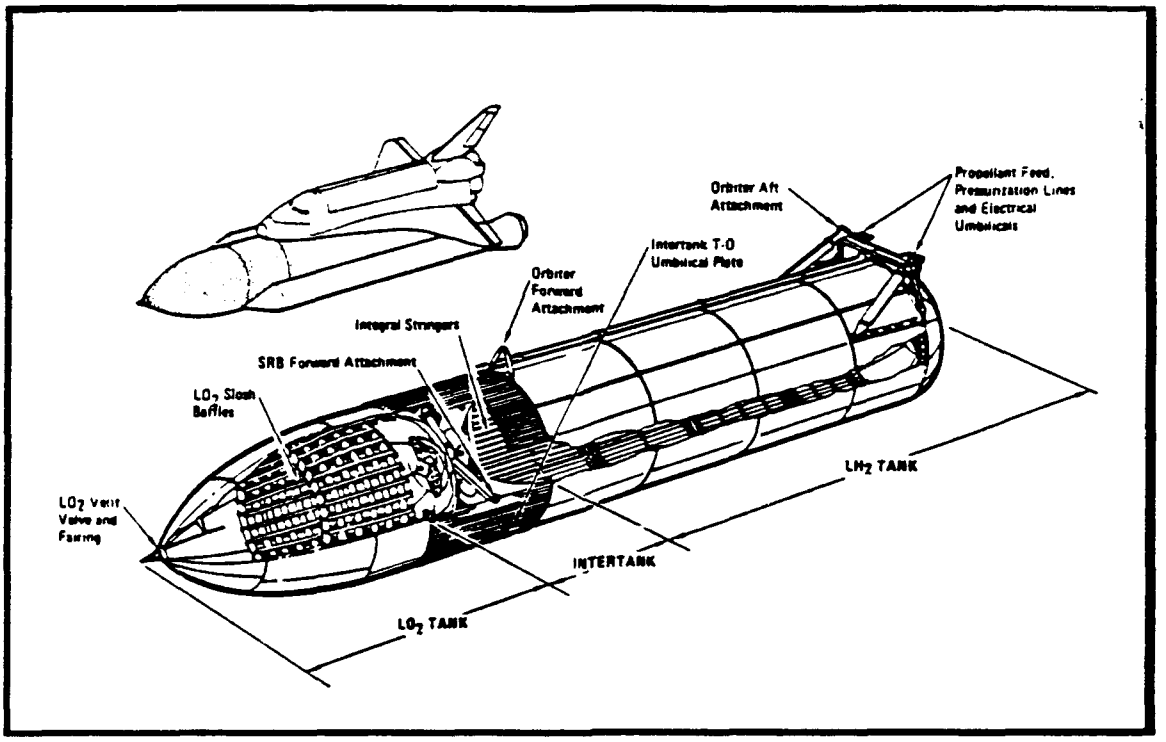

Fig. 2 Cut Away View of an STS External Tank

been proposed by government and private industry groups. The capabilities provided by the ET not available elsewhere include large relatively inexpensive masses of aluminium (in excess of 53,000 lb per tank) in earth orbit, large factory tested pressure vessels, and large enclosed volumes ready for use in orbital storage until needed. The tank could be disassembled in orbit and used as parts for a large space structures. These structures could be used to build the basis for many different types of space facilities, such as a space station, or an on orbit fuel station, or even as part of an interplanetary spacecraft. It is also possible

to melt the tank aluminum for on-orbit manufacturing uses. Additionally, each ET would still contain an average of 15,000 lb of residual cryogenic fuel and oxidizer when it arrives in orbit. This is due to reserve, pressurization, and ullage requirements (8:II-5). This liquid hydrogen and liquid oxygen can be scavenged from the tank after launch for a variety of uses on-orbit. Both the liquid hydrogen tank and the liquid oxygen tank are capable of on-orbit storage of cryogenic fuels and other volatiles. The potential uses of the ET connected to a tether range from momentum exchange with the shuttle to electrical power generation with a conducting tether. However, prior to utilizing an external tank in space, a major obstacle must be addressed; how to prevent it from decaying out of orbit prematurely.

At the present time, the primary obstacle to the proposed use of the ET in low Earth orbit (LEO) is orbital lifetime. All objects in LEO experience atmospheric drag. Work is required to push the air molecules out of the way which reduces the kinetic energy of a satellite. This effect causes the orbit to shrink where the orbital velocity requirement is greater; around the perigee point. This increase in speed combined with the higher density of the lower atmosphere results in an increased drag force. And the cycle continues until the satellite completely decays (27:296). This phenomena was observed with the Skylab space

station. Skylab's orbit decayed due to increased solar activity that adversely affected the density of the atmosphere. The additional drag on the spacecraft led to its earlier than planned re-entry (26:39). An orbiting external tank could suffer the same fate. An unexpected re-entry would defeat the purpose for bringing the ET into space and produce the possibility of raining large pieces of a disintegrating tank over populated areas. On the shuttle mission that launched the Hubble Space Telescope, the re-entry of the ET was observed by the USAF Maui Optical Station in Hawaii. The tank exploded and broke up at high altitude, however several large pieces of it, weighing several hundred pounds survived re-entry and hit the ocean (3:52). If this would have happened over land the results could have been disastrous. Presently, the launch trajectory of the STS and the jettisoning of the ET are planned to provide a "controlled" re-entry of the ET during the first orbit. To prevent an ET that was taken into orbit from re-entering prematurely some form of active propulsion utilizing small thrusters (or an alternate form of orbital maintenance such as momentum transfers involving tethers) is required. But the first tanks taken into orbit may not be equipped with small thrusters to accomplish this task. And possibly, ET end-users would make use of the tank before it began a final, blazing plunge through the lower layers of the atmo-

sphere.

Therefore parking orbits must be found for the ET that will prevent it from early re-entry. The thrust of this study is to determine parking orbits for a single external tank, awaiting its future purpose, that are within the operating capability of the STS . For this investigation, these parking orbits will be defined by two criteria. First, the time horizon chosen is 90 days. This three month window is selected to represent the amount of time allowed for the ET to remain in its parking orbit before the end-users would make use of it. After which, (1) the tank could be disassembled, (2) it could be boosted to a higher orbit by a space tug or some sort of "strap on" propulsion system, (3) it could be incorporated into some type of structure that has an orbital maintenance capability such as a space station. Secondly, the maximum tolerable altitude loss by the ET over the 90 day period would be 25 kilometers. Any initial orbit that loses more than 25 km in perigee altitude would be considered unacceptable. These two assumptions produce a platform from which to answer the primary question: What are the lowest initial orbits for deploying the external tank sufficient to meet the parking orbit requirements?

To accomplish this the equations of motion (EOM) of an ET in low Earth orbit are numerically integrated for a given

set of initial orbital elements. Typical shuttle orbit parameters are used in the search for minimum parking orbits. Finally, various aspects of the orbit, and Earth's gravitational field and atmosphere are investigated to determine their relationship with orbital decay. Chapter IV details the results of this examination of an external tank in low Earth orbit.

II MATHEMATICAL MODEL

The mathematical model for this problem assumes both bodies closely follow paths according to two-body motion, with only minor deviations due to small perturbing forces. Additionally, the mass of the primary (Earth) will be assumed to be much greater than the mass of the secondary body (shuttle tank). This implies that the center of mass of the primary may be used as the center of mass for the system and that the effect of the secondary on the motion of the primary will be negligible. Now, the effects of a non-spherical Earth and other perturbing forces will be examined.

A body orbiting a spherical planet of homogeneous structure and with no outside environmental disturbances, would continue forever in an idealized Keplerian orbit; its orbital elements remaining constant at their initial values. In real celestial systems however, there are several interfering influences capable of perturbing the satellite's motion. They are:

1) the irregular shape and variable composition of the primary

2) the atmosphere of the primary

3) the magnetic field of the primary

4) solar radiation pressure

5) the gravitational fields of other nearby bodies

The effect a perturbing force has on a specific orbital element does not directly correspond to its magnitude. For instance, the Earth's gravitational attraction is on the order of one dyne, but because it is a conservative force, produces no appreciable long term perturbation upon a satellite's semi-major axis. However, it does produce both long and short term periodic variations in several of the orbital elements. Conversely, the atmospheric drag (on the order of 10^{-5} dyne) acting on a low orbit satellite causes a noticeable secular decrease in the semi-major axis (9:973).

In low Earth Orbit the two principal perturbations experienced by a body are caused by the irregularity of the Earth's gravity field and atmospheric drag. Third body effects (from the Sun and Moon) have a negligible effect on the orbital decay problem and will not be considered in this study (20:52). Solar radiation can produce marked effects on a satellites orbit if the density of the satellite is small, as in the case of balloon satellites such as Echo I (24:216). However, the density of an external tank is large enough to disregard this perturbing force. If the satellite has metal in its construction the Earth's magnetic field

induces eddy currents in the satellite and a slight retardation acts on the satellite. The changes in the orbit due to this are very small compared to the effects of other perturbations (24:216). Because of the magnetic fields small effect and the short time span to be studied this effect will be also neglected. The next two sections will develop expressions for the two main perturbations which are to be considered in this study (i.e. gravity field irregularities and atmospheric drag).

Gravity Model

The Earth's gravitational field is the dominant controller of an low Earth orbiting satellite. However, as experienced by a satellite in low orbit, Earth's gravitational field does not exhibit spherical symmetry. The rotation of the earth causes it to bulge at the equator by almost 20 km, and irregular placement of continental land masses which are separated by ocean basins all contribute to Earth's deviation from a Newtonian point mass and produce a non-spherical shape to Earth's gravitational field (24:204). As a satellite orbits the globe it encounters a variable force of gravity leading to changes in its orbital parameters. A formulation is needed to model this perturbing effect.

The attractive force between two bodies of mass M and m, separated by distance r, is governed by Newton's universal law of gravity:

$$F = G\frac{Mm}{r^2} \tag{1}$$

Where G is the universal gravitational constant. Combining Eq (1) with Newton's second law

$$F = ma \tag{2}$$

provides the acceleration of body m with respect to the two-body center of mass (which, as previously stated conveniently coincides with the center of mass of the primary):

$$a = \frac{GM}{r^2} \tag{3}$$

Instead of working with an acceleration in determining the gravitational disturbance, it is simpler to convert the acceleration to a vector and express this vector as a potential function (15:1).

An equivalent vector is obtained by representing the acceleration as a gradient of a scalar, V, defined as the potential (per unit mass):

$$\bar{a} = \nabla V \tag{4}$$

where

$$V = \frac{GM}{r} \tag{5}$$

Using a Cartesian coordinate system, with its' origin at the center of mass of M, the acceleration can be represented as

$$\bar{a} = \nabla V = \frac{\partial V}{\partial x}\hat{i} + \frac{\partial V}{\partial y}\hat{j} + \frac{\partial V}{\partial z}\hat{k} = -GM\frac{x}{r^3}\hat{i} - GM\frac{y}{r^3}\hat{j} - GM\frac{z}{r^3}\hat{k} \tag{6}$$

The second derivative of the potential is then

$$\frac{\partial^2 V}{\partial i^2} = GM\left(-\frac{1}{r^3} + \frac{3i^2}{r^5}\right) \tag{7}$$

Combining the three ccmponent second derivatives gives the Laplacian

$$\nabla^2 V = \frac{\partial^2 V}{\partial x^2} + \frac{\partial^2 V}{\partial y^2} + \frac{\partial^2 V}{\partial z^2} \tag{8}$$

or

$$\nabla^2 V = GM\left(-\frac{3}{r^3} + \frac{3(x^2+y^2+z^2)}{r^6}\right) \tag{9}$$

In Poisson's fundamental partial differential equation for gravitational fields (6:277,279):

$$\nabla^2 V = -4\pi G\rho \tag{10}$$

where ρ is defined as the density of M. For a satellite orbit outside the body M, the density equals zero which leads to Laplace's equation:

$$\nabla^2 V = 0 \tag{11}$$

Since the body M (Earth, in this case) is basically spherical in shape, transforming Eqs (7) and (9) into spherical coordinates will aid in the derivation. The result of this transformation is

$$r^2\nabla^2 V = \frac{\partial}{\partial r}\left(r^2\frac{\partial V}{\partial r}\right) + \frac{1}{\cos\phi}\frac{\partial}{\partial\phi}\left(\cos\phi\frac{\partial V}{\partial\phi}\right) + \frac{1}{\cos^2\phi}\left(\frac{\partial^2 V}{\partial\lambda^2}\right) = 0 \tag{12}$$

where

r = radial distance from origin

ϕ = latitude

λ = longitude

Any solution, V, to Eq (12) is referred to in literature as a spherical harmonic. However, a closed form solution does not exist for this type of expression. Instead, if a solution of the following form is assumed (15:4):

$$V = V(r,\phi,\lambda) = R(r)\Phi(\phi)\Lambda(\lambda) \tag{13}$$

it can be inserted into Eq (12), which causes the partial derivatives to become total derivatives since each of the functions R, Φ, and Λ are only functions of one variable. Dividing this equation by $R\Phi\Lambda$ gives

$$\frac{1}{R}\frac{d}{dr}\left(r^2\frac{dR}{dr}\right)+\frac{1}{\Phi\cos\phi}\left(\cos\phi\frac{d\Phi}{d\phi}\right)+\frac{1}{\Lambda\cos^2\phi}\left(\frac{d^2\Lambda}{\lambda^2}\right)=0 \tag{14}$$

Since the first term of Eq (14) is the only term that is a function of r, it must be constant. Assuming this constant is -l(l+1), the solution to R is

$$R = Ar^l + Br^{-l-1} \tag{15}$$

where A and B are arbitrary constants. Substituting this result back into Eq (14) and multiplying by $\cos^2\phi$, the term containing Λ can be separated from the other terms. Letting the this term equal the constant $-m^2$ and solving for λ gives

$$\Lambda = C\cos m\lambda + S\sin m\lambda \tag{16}$$

where C and S are arbitrary constants. When separating the Φ term from the potential the resulting equation is a type know as Legendres' Equation, and is solved by assuming Φ is represented by a power series in μ. Where $\mu = \sin\phi$. The solution of this is called an Legendre Associated Function (15:5).

$$P_{lm}(\sin\phi) = \cos^m\phi \sum_{t=0}^{k} T_{lmt} \sin^{(-l-n-2t)}\phi \tag{17}$$

where

$$T_{lmt} = \frac{(-1)^t(2l-2t)!}{2^l t!(l-t)!(l-m-2t)!} \tag{18}$$

$$k = intger\ \ part\ \ of\ \ \frac{(l-m)}{2} \tag{19}$$

Finally, any combination of Eq (15), (16), and (17) may be multiplied together, so long as the values of l and m match. Also, any combination of $R(r)\Phi(\phi)\Lambda(\lambda)$ may then be added together. The result is

$$V = \sum_{l=0}^{\infty} \sum_{m=0}^{n} \frac{1}{r^{l+1}} P_{lm}(\sin\phi)[C_{lm}\cos m\lambda + S_{lm}\sin m\lambda] \tag{20}$$

The constants C_{lm} and S_{lm} characterize the mass distribu-

tion of body M and the terms l and m are the order and degree of the potential. To represent a model of the Earth's geopotential, Eq (20) can be expressed as

$$V = \frac{\mu}{r}\sum_{l=0}^{\infty}\sum_{m=0}^{l}\left(\frac{R_e}{r}\right)^l P_{lm}(\sin\phi)[C_{lm}\cos m\lambda + S_{lm}\sin m\lambda] \qquad (21)$$

By including the Earth's gravitational parameter μ and equatorial radius R_e. C_{lm} and S_{lm} are redefined from Eq (20) to make them dimensionless (6:284). When m = 0 Eq (14) simplifies to

$$V = \frac{\mu}{r}\sum_{l=0}^{\infty}\left(\frac{R_e}{r}\right)^l P_{l0}(\sin\phi)C_{l0} \qquad (22)$$

The geopotential components of this equation are referred to as zonal harmonics and are due to variations in meridian ellipticity. When m = 1, the components of equation 15 are called sectoral harmonics and are caused by longitudinal variations in the shape of the Earth. Tesseral harmonics are concerned with cases where m < l. (also for all m > 1, the associated Legendre function $P_{lm}\sin\phi$ equates to zero). Values of the potential coefficients C_{lm} and S_{lm} for Earth were determined from repeated observations of various satellite orbits. By studying the long term perturbations, the coefficients of the zonal harmonics have been found and the sectoral and

tesseral harmonic coefficients were determined from analysis of short term orbit perturbations. These geopotential constants have been calculated through many orders and degrees (6:271).

It is of interest to note that, when both l and m equal zero, Eq (21) reduces to the basic potential for a spherically symmetric Earth:

$$V = \frac{\mu}{r} = \frac{GM}{r} \tag{23}$$

meaning $C_{0\,0}=1$ and $S_{0\,0}=0$. This study will use a model of order 2 and a degree of zero for the Earth's potential. Studies have shown the short term perturbations caused by higher harmonics have little affect on the orbital decay problem (6:285). Therefore, Eq (21) can be reduced to:

$$V = \frac{\mu}{r}\left(1 + \left(\frac{R_e}{r}\right)^2 P_{20}(\sin\phi)C_{20}\right) \tag{24}$$

Considering the second term in Eq (24), the part of the potential due to the Earths oblateness, and transforming this back to Cartesian coordinates, and then taking the gradient of this potential will give the perturbing acceleration of the secondary body caused by the equatorial bulge (17:3-3).

$$\nabla V_2 = \bar{a}_{J_2} = a_x\hat{i} + a_y\hat{j} + a_z\hat{k} \tag{25}$$

where

$$a_x = -\frac{3}{2}\left(\frac{J_2R^2}{r^6}\right)\mu x\left(1-\frac{5z^2}{r^2}\right) \tag{26}$$

$$a_y = -\frac{3}{2}\left(\frac{J_2R^2}{r^6}\right)\mu y\left(3-\frac{5z^2}{r^2}\right) \tag{27}$$

$$a_z = -\frac{3}{2}\left(\frac{J_2R^2}{r^5}\right)\mu z\left(3-\frac{5z^2}{r^2}\right) \tag{28}$$

$$J_2 = -C_{20} = 0.0010826271$$

Air Drag

As a body passes through the rarified regions of the upper atmosphere it is subjected to an aerodynamic force which perturbs its orbital motion. This force can be separated into two quantities; the component opposite the direction of motion called drag, and the component perpendicular to the body's flight path. This second quantity generally does not pass through the satellite's center of mass and can subsequently be divided into a lifting force and a turning moment about the center of mass (see Figure (3a)). For an uncontrolled satellite, the turning moment will normally be a destabilizing one, tending to make the satellite tumble end over end (16:13). In this study, the ET will be placed in orbits where another torque acting on the ET dominates over the

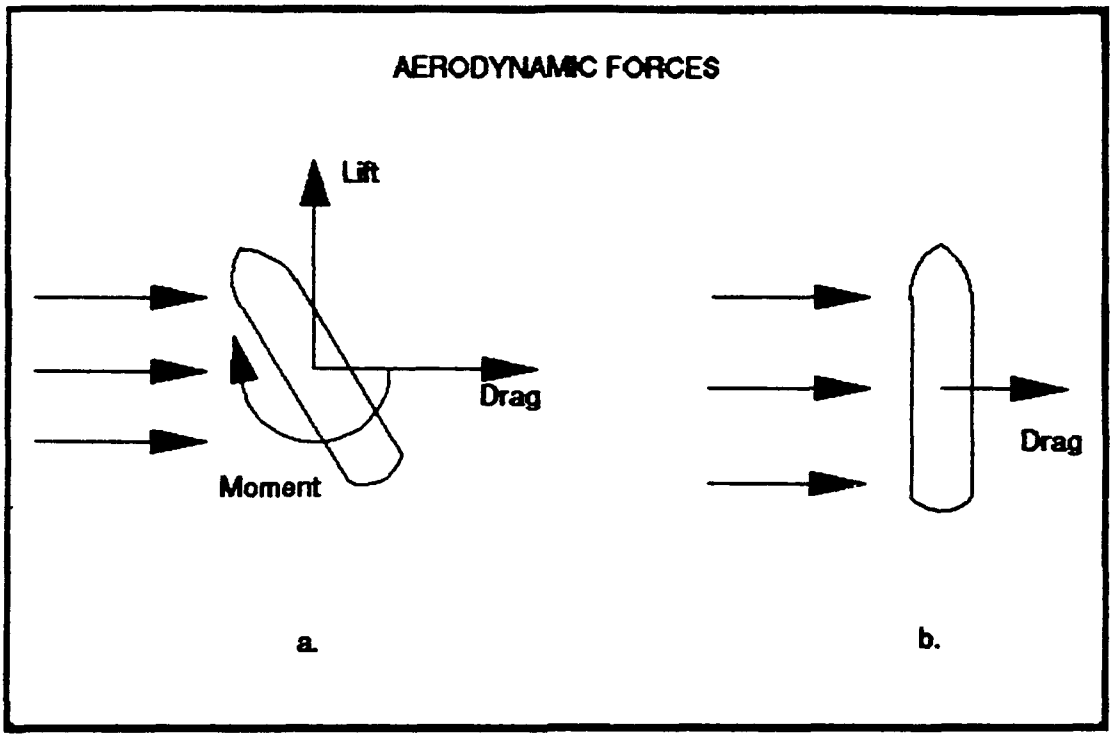

Fig. (3) Aerodynamic Forces on an ET

aerodynamic torque. This other torque, the gravity gradient, prevents the ET from tumbling (see in the section on surface area for a further explanation of the gravity gradient). Since the gravity gradient holds the ET perpendicular to the relative wind (see Figure (3b)) the lift that would be generated by the ET would be negligible and will be ignored in this analysis. This leaves drag as the only aerodynamic force to consider in the study of an ET in low Earth orbit.

In aerodynamics the conventional drag equation is (16:12)

$$D = \frac{1}{2}\rho A C_d V^2 \tag{29}$$

where

D = drag force

ρ = atmospheric density

Cd= drag coefficient

A = satellite area normal to the air flow

V = satellite velocity relative to the atmosphere

This formulation of the drag equation can alternately be expressed as a drag deceleration:

$$a_{drag} = \frac{D}{m} = \frac{1/2 C_d A}{m}\rho V^2 = B\rho V^2 \tag{30}$$

where the ballistic coefficient, B, is a convenient method of combining the satellite parameters A, m, and C_d into one term for parametric studies. The elements of the drag equation will now be examined with respect to an Earth orbiting spacecraft.

Atmospheric Density. The major property of the Earth's atmosphere important to low orbit satellites is its' density. Two basic equations play a role in deter-

mining air density as a function of altitude. First, the perfect gas law relates the atmospheric properties of pressure p, density ρ, and temperature T:

$$p = \rho \frac{R}{M} T \tag{31}$$

where

R = universal gas constant

M = mean molecular weight of the atmosphere

The second expression to consider is the hydrostatic equation which relates the rate of change in pressure to the increased weight of the supported atmosphere:

$$dp = -\rho g dr \tag{32}$$

where g = gravitational acceleration (29:4). Logarithmic differentials of Eq (31) give

$$\frac{d\rho}{\rho} = \frac{dp}{p} - \frac{dT}{T} \tag{33}$$

When combined with Eq (32) this produces

$$\frac{d\rho}{\rho} = -\left(\frac{gM}{RT} + \frac{1}{T}\frac{dT}{dr}\right)dr \tag{34}$$

or

$$\frac{d\rho}{\rho} = -\beta dr \tag{35}$$

where β is the terms in the brackets of Eq (34) and represents the inverse of the scale height. Integrating Eq (35) and substituting H for $\frac{1}{\beta}$ yields

$$\rho = \rho_o \exp\left\{-\frac{(r - r_o)}{H}\right\} \tag{36}$$

where

r = altitude

r_o = reference altitude

ρ_o - density at reference altitude

The scale height is the vertical distance in which the air density changes by a factor of exponential e. The value of H is dependent on altitude, increasing slowly with height.

Several different density profiles can be considered depending on assumptions on β (27:4-5):

1) Strictly exponential atmosphere: β is assumed constant throughout the atmosphere.

2) Locally exponential atmosphere: β is constant

over a small altitude window.

3) βr - constant atmosphere: The dimensionless quantity βr remains constant.

4) Isothermal atmosphere: The temperature is considered constant through an altitude interval so that $dT/dr = 0$ and βr becomes $(gM/R)T$. For an inverse-square gravitation field

$$g = g_o\left(\frac{r_o}{r}\right)^2 \tag{37}$$

leads to the quantity βr^2 being constant.

All four profiles use the density exponential function of Eq (36). For the purposes of this study the second case, the locally exponential atmosphere, will be utilized.

In actuality, the density in the upper regions of the atmosphere is an exceedingly variable quantity with solar activity being the main cause of this irregularity. Observations of the orbits of early satellites were used in analyzing these atmospheric density fluctuations.

One basic air density difference exists between the sunlit and nighttime sides of the Earth. This hump of density, the diurnal bulge, occurs about two hours after midday. The change in density between day and night is small for altitudes of 250 km and below, however, above

this altitude large variations can take place. For example, at 600 km, the maximum daytime density is about 8 times greater than the nighttime minimum (16:18).

Along with this daily density variation there are four other solar influences. First, there exists an irregular day to day deviation in density due to ephemeral solar disturbances such as short term flares. A second density variation occurs with a 27 day cycle. This effect is due to the axial rotation of the Sun with respect to the Earth. Next, the properties of the atmosphere also respond to the 10 to 11 year sunspot cycle. Lastly, a seasonal oscillation in density appears with a minimum occurring during July and January, and a maximum appearing in October and April. These seasonal effects are largely due to the Earth's orbit around the Sun. A model of the atmosphere containing all of these effects, called a dynamic atmosphere, would be very complex (16:18-19).

For perturbations caused by the Earth's atmosphere this investigation uses a simple exponential density model as expressed by Eq (36). Reference (22) is the source of Earth's atmospheric density and scale height values at various reference altitudes. This type of atmosphere model is called the "static atmosphere." Instead of modeling the changes in atmospheric density

caused by the Sun, it describes "average" atmospheric properties which represent a mean value of the diurnal bulge, seasonal, and other solar caused variations detailed above. This model is then time independent and only depends on altitude.

The greatest limitation in using this atmospheric model is in the assumption of spherical symmetry. As expressed, the air density is only a function of the radial distance from the center of the Earth. However, the Earth is an oblate spheroid and hence produces a latitude effect to the atmospheric properties. Given the ellipticity, ϵ, of the Earth an approximate geodetic altitude, h_g, may be calculated by

$$h_g = r - \sqrt{\frac{R^2(1-\epsilon^2)}{1-\epsilon^2\cos^2\delta}} \tag{38}$$

where δ is the geocentric latitude and R is the equatorial radius of the Earth. To obtain the true geodetic altitude requires the solution of a fourth order polynomial. However, this approximate geodetic altitude is quite adequate in evaluating density of the atmosphere above an elliptical Earth (17:3-5). This atmospheric oblateness and aforementioned solar activity cause the main distortions from spherical symmetry. More complex models of the atmosphere have been devised to account for these

variational effects. However in order to keep the model simple (and thereby reduce computer time) the static atmosphere is used.

Satellite Velocity. The component V, in the atmospheric drag equation represents the satellite's velocity relative to the atmosphere. With v_a being the velocity vector of the air and v the satellite's velocity vector (both with respect to an Earth fixed coordinate frame)

$$\bar{V} = \bar{v} - \bar{v}_a \tag{39}$$

Assuming the atmosphere rotates with the Earth, then the velocity of the atmosphere, at any given point, can be found by taking the cross product

$$\bar{v}_a = \bar{\omega} x \bar{r} \tag{40}$$

where $\bar{\omega}$ is the angular velocity vector (rotation rate) of the Earth, and $\bar{r}$ is the position vector of the part of the atmosphere whose velocity is being determined. In the case of this study the position vector for the external tank will be used. Using $\bar{r}$ in spherical coordinates

$$|\bar{v}_a| = v_a = r\omega\cos\phi \tag{41}$$

where ϕ is the geocentric latitude. Squaring Eq (39) yields

$$V^2 = v^2 + v_a^2 - 2vv_a\cos\gamma \tag{42}$$

where γ is the angle between v_a and v. Examining triangle SNL in Figure (4), the equation (determined from spherical trigonometry)

$$\cos\gamma^* \cos\phi = \cos i \tag{43}$$

where i is the inclination and γ^* is the angle between $\bar{v}_a$ and the horizontal component v_h of $\bar{v}$, is obtained. For small eccentricities, a satellite travels nearly horizontal through the atmosphere. A very small error, less than one percent, results if the angle γ is taken as the angle γ^* (16:23). Using this approximation and substituting Eq (41) into Eq (43) results in

$$v_a\cos\gamma = r\omega\cos i \tag{44}$$

Substituting this result into Eq (42) produces

$$V^2 = v^2\left(1 - \left(\frac{r\omega}{v}\right)\cos i\right)^2 + r^2\omega^2(\cos^2\phi - \cos^2 i) \tag{45}$$

Further assumptions may be made to simplify this expression. First, the $r^2\omega^2$ term can be neglected due to $r^2\omega^2$ being three orders of magnitude less than V^2, since ω is of the same order as Earth's angular velocity. For small eccentricities r and v remain relatively constant, therefore these variables may be replaced by initial values r_o and v_o. Furthermore, the constant i_o may replace i due to the orbit's inclination changing very little during the short time period considered by this study (16:24). Eq (45) may then be recast as

$$V^2 = v^2\left[1 - \left(\frac{r_o\omega}{v_o}\right)\cos i_o\right]^2 \tag{46}$$

The atmospheric drag equation may now be written as

$$D = \frac{1}{2}\rho v^2 F C_d A \tag{47}$$

where

$$F = \left[1 - \left(\frac{r_o\omega}{v_o}\right)\cos i_o\right]^2 \tag{48}$$

The quantity F represents the effect of atmospheric rotation on the drag force. Assuming ω is equal to Earth's rotation rate, F will normally lie between 0.9 and 1.1, and although the effect of atmospheric rotation on drag

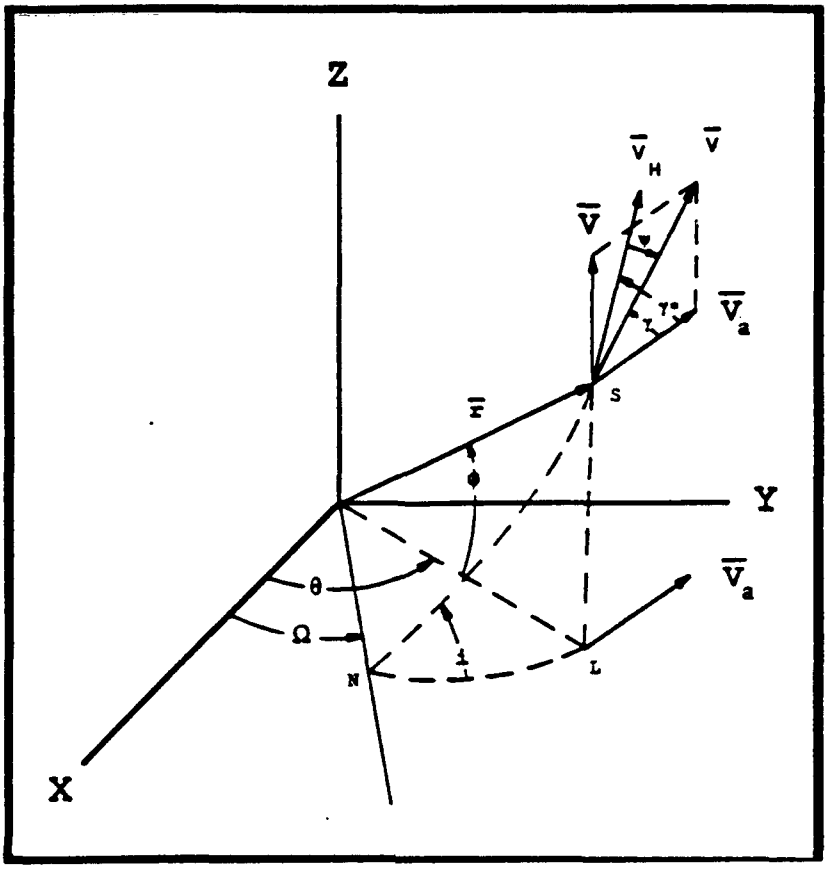

Fig. (4) Atmospheric Velocity Representation

is slight it is not inconsequential (16:25).

Coefficient of Drag. The drag coefficient, Cd, is an important element in the aerodynamic drag equation. While a more accurate value of the total aerodynamic force may be determined using a differential equation it is more convenient to use the drag coefficient in the orbital analysis. When working with a coefficient of drag several assumptions must be made concerning the

atmospheric molecules (16:14-15):

1) The satellite is considered to be stationary with respect to the air molecules flowing past.

2) The molecules are assumed to impinge on the satellite, be retained temporarily on its surface, and then re-emitted.

3) the collisions between incident and re-emitted molecules are neglected.

Several factors come into play in calculating the drag coefficient. The first parameter is the flow regime through which the satellite moves. This flow type is determined by the Knudsen number, defined as the ratio of mean free path of atmospheric molecules to the characteristic linear dimension of the satellite. Two hundred kilometers above the Earth the ordinary continuous flow of conventional aerodynamics no longer applies because of extremely low air density. This region is called free molecular flow and has a Knudsen number of 10 or greater. When a satellite is in this flow regime its' drag coefficient is dependent on the molecular speed ratio. This is the ratio of satellite speed to most probable molecular speed. For altitudes below 700 km this speed ratio always exceeds 5. This implies the random thermal motion of the atmospheric molecules may be ignored (i.e. the

flow is hyperthermal) (2:931).

Another factor is the mechanism of molecular reflection. The energy exchange between the atmosphere molecules and the satellite is dependent on the direction of the reflected molecules and their speed. It is assumed the air molecules impinging on the satellite's surface do not reflect specularly , but instead attach themselves to the outer layer of the surface for a period of time before being re-emitted. During this period the molecules 'forget' their original direction of motion and are re-emitted diffusely. This diffuse reflection is strongly contingent upon the nature of the satellite's surface and its structure (2:931).

The speed of the re-emitted molecules is determined by their kinetic temperature. During the period of attachment the molecules also 'forget' their original temperatures. By how much they 'forget' is uncertain and leads to the accommodation coefficient, defined as (16:16):

$$\alpha = \frac{T_i - T_r}{T_i - T_s} \tag{49}$$

where

Ti = original molecular temperature

Tr = re-emitted molecular temperature

Ts = satellite surface temperature

theoretical values of the accommodation coefficient are very difficult to determine. Many assumptions must be made concerning the gas molecules and their interaction with the satellite's outer surface. Low values of the coefficient are assumed to be appropriate (2:931,934). This implies higher drag coefficients. Reference 15, assumes from "conflicting and rather unsatisfactory" experimental results that the accommodation coefficient is nearly 1.0, but admits this assumption may be wrong.

Reference 3 presents a graph of drag coefficients versus accommodation coefficients for a circular cylinder with its axis perpendicular to the direction of motion. Hyperthermal free molecular flow and a T_s/T_i ratio of 0.006 are both assumed (2:939). See Figure (5). The upper line is a plot of

$$C_d = 2(1 + r\pi/6) \tag{50}$$

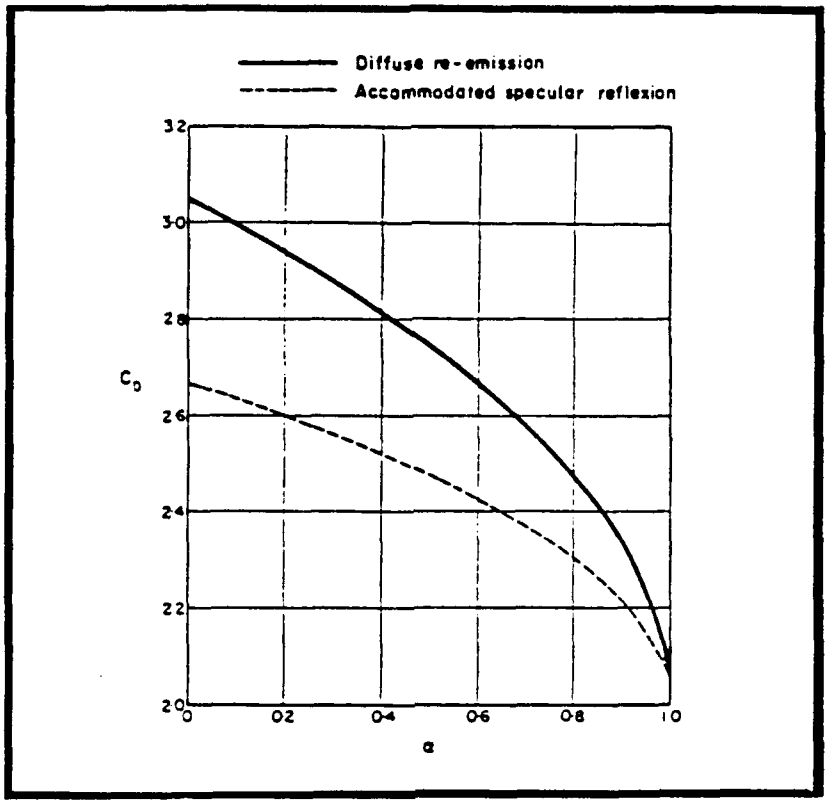

Fig. (5) Drag Coefficients for Cylinders

where diffuse re-emission is assumed. The term r here is a ratio of the speed of a re-emitted molecule, V_r, to the speed of an incident molecule, V_i, and is related to α by

$$r = \frac{V_r}{V_i} = \left[1 + \alpha\left(\frac{T_s}{T_i} - 1\right)\right]^{1/2} \qquad (51)$$

The ratio T_s/T_i is very small so r can be approximated by

$$r = [1 - \alpha]^{1/2} \qquad (52)$$

The last factor to consider in determining the drag coefficient is the satellite's dynamics and orientation to the atmospheric flow. For a cylinder tumbling end over end

$$C_d = 2\left[1 + \left\langle \frac{\pi^2(l+d)}{6(l+d)} \right\rangle r\right] \tag{53}$$

where

l = cylinder length

d = cylinder diameter

This equation for Cd produces similar results for various values of l/d (2:940). However, if a gravity gradient attitude is used for the ET the drag coefficient may be obtained from Equation (50). From this it was determined that an external tank would have a drag coefficient of 2.4.

Satellite Area. The projected area normal to the free molecular flow of Earth's upper atmosphere also affects the drag force experienced by the satellite. The size of this area depends upon the orientation of the satellite as it orbits the Earth. Ideally, the ET should have its smallest cross-section pointing into the air flow, thereby minimizing drag. However, this attitude, with the long axis of the ET almost parallel to the

Earth's surface, is unstable and would require some form of attitude control system in order to be maintained. Since only a simple uncontrolled ET is to be studied, only stable attitudes for an ET must be examined.

Two main torques act on a vehicle in low Earth orbit; a gravity gradient torque and an aerodynamic torque. The gravity torque arises from the slightly different attraction of gravity across the vehicle. This torque will tend to point the long axis of the vehicle towards the center of the Earth. If the ET is released from the orbiter in this attitude, with no initial angular momentum, it will remain in this configuration until the aerodynamic forces become dominant. The aerodynamic torque will cause the ET to spin about its minor axis.

However, a satellite would not remain in these constant area positions relative to the flow. The ET's orbital dynamics may alter the size of the projected area. Below 370 km aerodynamic torques dominate an ET's dynamics while above 555 km the gravity gradient torques are the major influences. Between these altitudes both space torques can interact to cause an unstable disturbance in the satellite's orientation (19:2200).

If a gravity gradient attitude is assumed for an orbiting ET this would present a constant projected area to the relative wind. If a tumbling attitude, caused by

the aerodynamic torque, is assumed the projected area would be constantly changing. However, the average value of the projected area for a tumbling satellite would be less than the constant value from the gravity gradient attitude. Since the orbital altitudes of concern fall within the "gray" area where neither torque clearly dominates, a conservative approach will be taken. For the purpose of this study it will be assumed that the ET maintains a gravity gradient attitude; the worst case.

Equation of Motion

The primary assumption in the mathematical model is that both bodies travel in two-body motion with only minor deviations caused by perturbing forces. Therefore, the first step in setting up the equation of motion of the secondary body is to derive the equation for a pure two-body motion. The first assumption in the two-body problem is that no other forces are acting on these bodies (other than the gravitational attraction between them). Next, it is assumed that these bodies are spherically symmetric, which enables the bodies to be treated as though their masses were concentrated at their centers. The perturbing forces will account for the fact that the Earth is not spherical.

Applying Newton's second law to the secondary body (the external tank) yields

$$m\ddot{\mathbf{r}} = \sum \mathbf{F} \tag{54}$$

where r is the distance between the center of masses of the two bodies, and $\sum F$ is the summation of all forces acting on the ET (in this case is only gravity). Substituting Newton's law of universal gravitation into Eq (54) results in

$$m\ddot{\mathbf{r}} = -\frac{GMm}{r^2}\left(\frac{\mathbf{r}}{r}\right) \tag{55}$$

simplifying

$$\ddot{\mathbf{r}} = -\frac{\mu}{r^3}\mathbf{r} \tag{56}$$

where $\mu = GM$. This is the equation of motion for an idealized two-body system (24:69-70). The perturbations must be added in to make the math model follow the actual motion of the bodies. For the two-body problem with perturbations, the equation would be

$$\ddot{\mathbf{r}} = -\frac{\mu}{r^3}\mathbf{r} + \mathbf{a}_{perturbations} \tag{57}$$

where a_p are the perturbing accelerations. Substituting the results of the previous two sections yields

$$\ddot{\bar{r}} = -\frac{\mu}{r^3}\bar{r} + B\rho V^2\left(\frac{\bar{v}}{v}\right) + \bar{a}_{J_2} \tag{58}$$

which is the final form of the equation of motion for this study.

III METHOD OF IMPLEMENTATION

To solve the external tank problem a special perturbation technique was used. The simplest and most straight forward of all perturbation methods is Cowell's method. In this method one simply writes the equations of motion for the body being studied, including all the perturbations, and then integrates it step by step numerically. To apply Cowell's method, the equation of motion first have to be separated into three scalar equations, and then broken down into a set of six first order differential equations. Expressing these equations in rectangular coordinates:

$$\dot{x} = V_x \tag{59}$$

$$\dot{y} = V_y \tag{60}$$

$$\dot{z} = V_z \tag{61}$$

$$\ddot{x} = \dot{V}_x = -\mu \frac{x}{r^3} + a_{J_2} + a_{drag} \tag{62}$$

$$\ddot{y} = \dot{V}_y = -\mu \frac{y}{r^3} + a_{J_2} + a_{drag} \tag{63}$$

$$\ddot{z} = \dot{V}_z = -\mu \frac{z}{r^3} + a_{J_2} + a_{drag} \tag{64}$$

where $r = (x^2 + y^2 + z^2)^{1/2}$ and a_{J2} is from Eqs (26), (27), and (28), and a_{drag} is from Eq (47). This set of coupled equations is then inserted into a numerical integrator.

The type of integrator used for this study was an

eighth order Runge-Kutta single step method with a variable

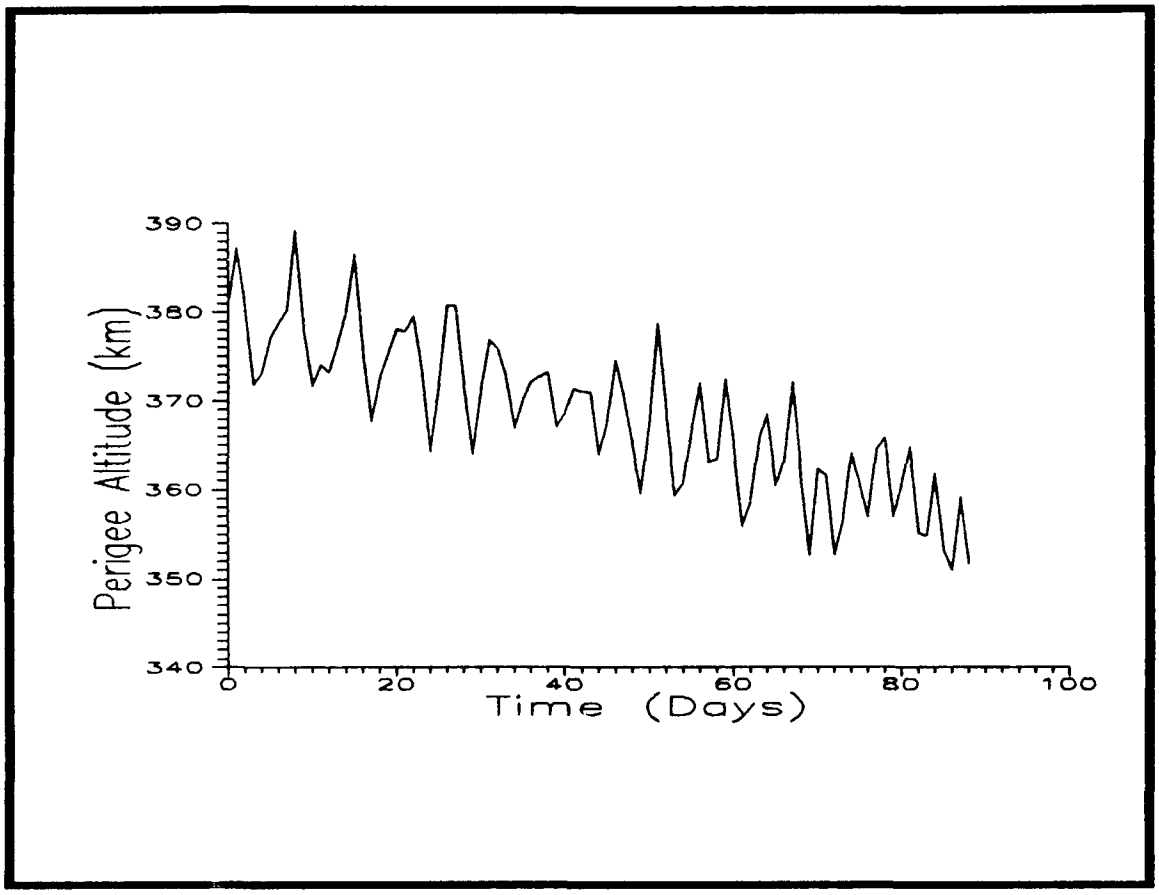

Fig. (6) Fluctuations in Perigee Altitude

step size. At each time step a set of Keplerian orbital elements is calculated. Since perturbations have been included in the EOM, the orbital elements will not remain constant, but are functions of time. The orbit described by these new elements is the two body orbit a satellite would follow if all the perturbations were removed at that moment. These orbital elements are called the "osculating" elements (24:159). The instantaneous values of these elements are

then used as a basis for calculating the satellite's orbit parameters at the next time step. For the external tank orbit study a two hour time step was employed which produced 12 orbit element calculations per day for the three month period.

The classical Keplerian elements (a,e,i,Ω,ω,M) are used to define the initial starting conditions of the orbiting external tank. The output of the numerical integration of the EOM is a time history of these elements. Since the equations of motion are integrated as rectangular coordinates, some form of transformation is needed to convert Keplerian elements to rectangular coordinates, and to convert rectangular coordinates back to Keplerian elements. Appendix 1 contains a complete description of the transformations used in this study.

The orbital elements for each time step must by converted to the perigee radius, r_p, by the expression (24:77):

$$r_p = a(1-e) \tag{65}$$

where a is the semi-major axis and e is the eccentricity. Subtracting the radius of the Earth from r_p gives the per-

igee altitude, which is the parameter needed to determine if the initial orbit fits the parking orbit criteria.

Figure (6) is a plot of the fluctuations in perigee

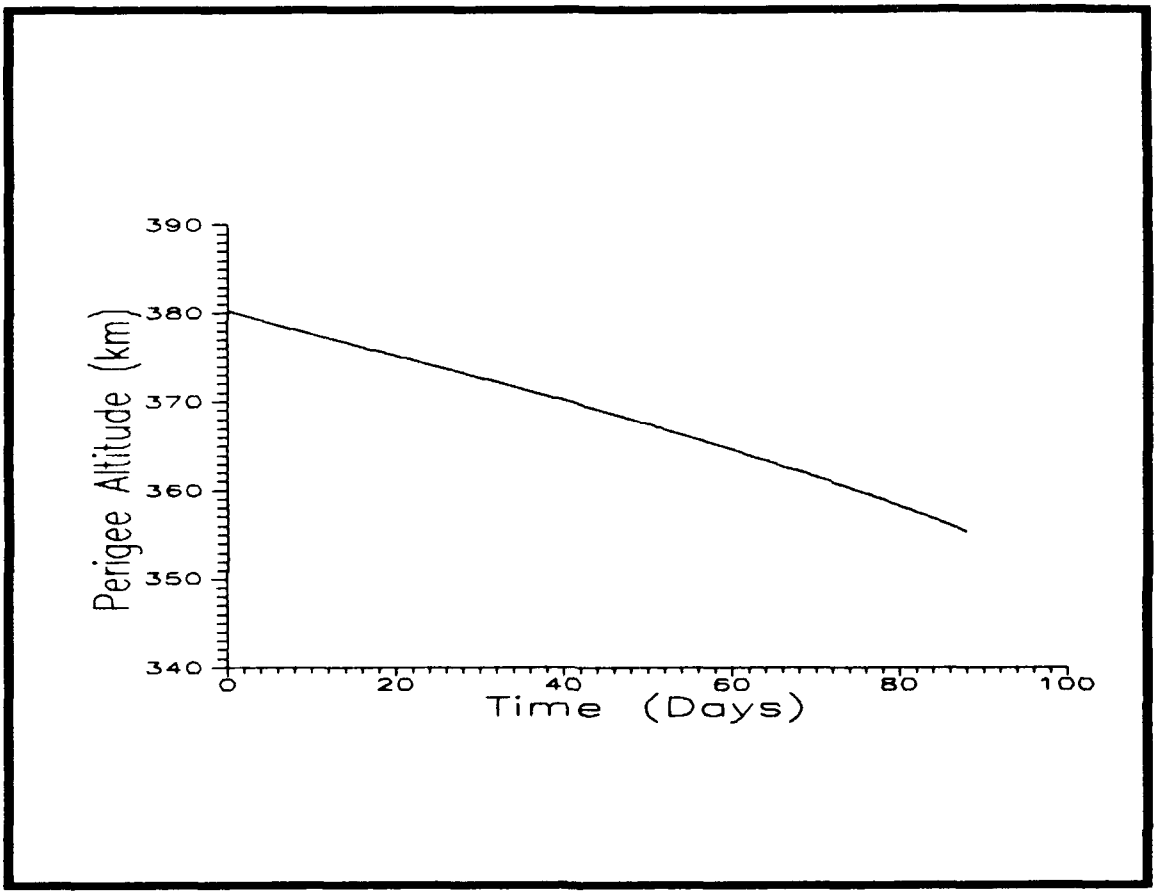

Fig (7) Fitting Curve to Perigee Fluctuations

altitude of an orbiting ET perturbed by both a gravity field and atmospheric drag. These fluctuations do not lead to a simple statement of the amount of altitude lost by the ET over the 90 day period. However, a regression function is used to perform a least squares fit to the data (see

Figure (7)). The type of curve employed was a third degree polynomial in time. It is therefore convenient to define the loss in perigee altitude as:

$$A_p = at + bt^2 + ct^3 \tag{66}$$

where t is time in days; A_p is perigee loss in kilometers; and a, b, and c are the polynomial coefficients generated by the curve fitting algorithm.

Different initial orbits were examined by varying their Keplerian elements, and then numerically integrating the corresponding EOM to find the resulting loss in perigee altitude after 90 days. During earlier orbit studies various values of the longitude of the ascending node, argument of perigee, and mean anomaly were evaluated and found to have no discernable effect on the 90 day altitude loss rate (20:33). For this reason, these three elements are set to zero for all initial orbits in this study. These three elements only determine the position of the ET within the orbit itself or with respect to the symmetrical axis of the Earth. While, the semi-major axis and eccentricity determine the size and shape of the orbit, and the inclination determines the orbits position with respect to the Earth's equatorial bulge.

These latter three Keplerian elements are varied to

produce initial orbits in which to park the ET. To keep within the operational capability of the STS the inclination was limited to a minimum of 28 degrees (approximate latitude of Kennedy Space Center) and a maximum of 63 degrees. Even though the shuttle is limited to a maximum inclination in the low fifties when taking off from the Cape, the limit was increased to 63 degrees to determine if the "critical" inclination would have an effect on the ET altitude loss.

IV RESULTS

A satellite in orbit around the Earth has six degree of freedom system. Therefore, it takes a six dimensional phase space to fully represent it. These different degrees of freedom may be represented by different sets of coordinates, such as Cartesian coordinates, the Keplerian orbital elements, the Delaunnay elements, or equinoctal elements. Each of these sets of coordinates have certain advantages, however, for visualizing what an orbit looks like the Keplerian elements are the best. Therefore, they will be used to describe the orbits in this study.

The problem is that there is no way to graphically represent a six dimensional phase space. Therefore a restriction is placed on the number of degrees of freedom. As stated previously, this study accomplished this by holding three of the elements equal to zero. Even though their values would change once an orbit was integrated, their initial values remained constant throughout the study. This reduced the phase space for initial orbits to three dimensions.

All of the orbits that lose 25 km in perigee altitude were graphed using a rectangular coordinate system. Where the axis are the semi-major axis, eccentricity, and

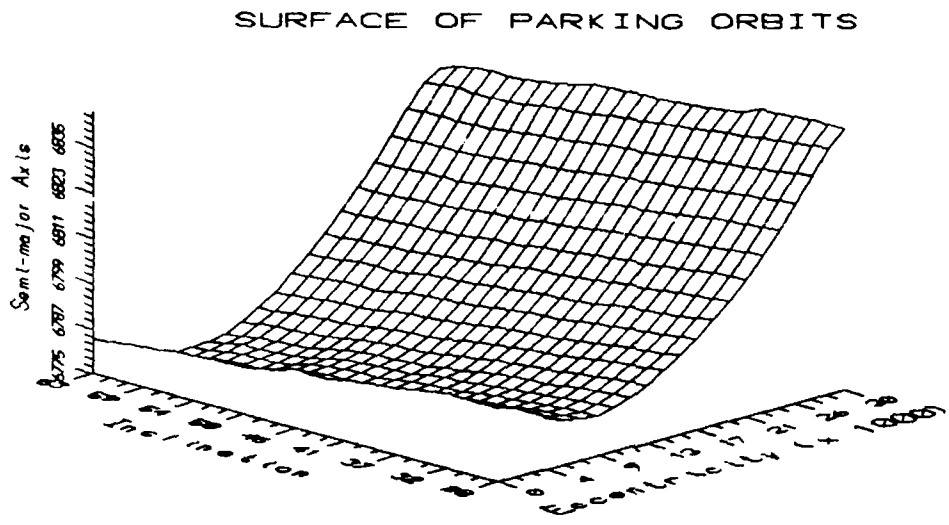

Fig. 8 Three Dimensional Plot of Orbits

inclination. A computer graphics program was used to derive a surface out of the data points (see Figure (8)). All orbits that are above this surface lose less than 25 km, and all orbits below it lose more than 25 km. To analyze this surface, the first step was to examine the effects of varying the eccentricity on the semi-major, while holding inclination constant. Next, the effects on the semi-major of varying the inclination, while holding eccentricity constant was examined.

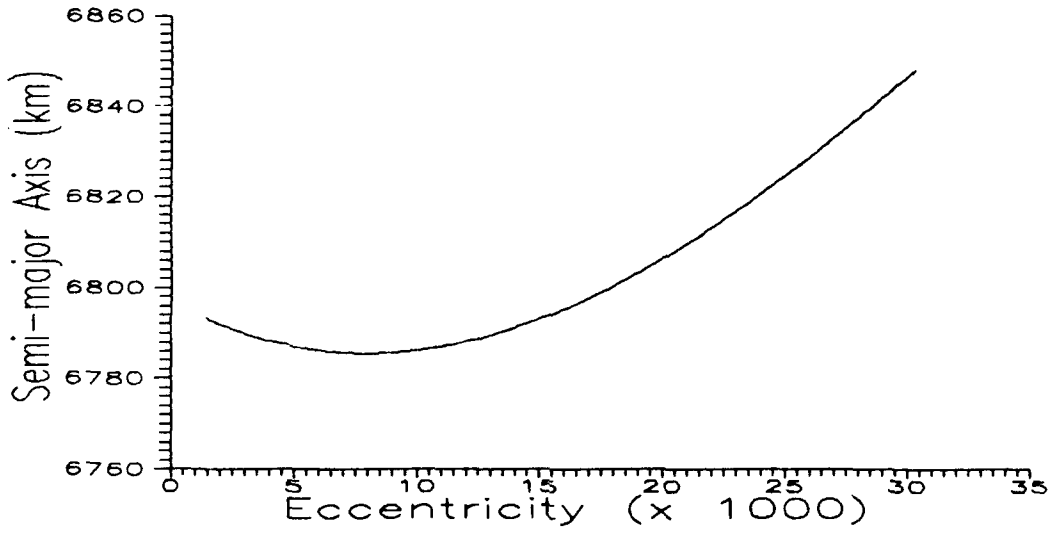

Fig. 9 Graph of Parking Orbits for I=28°

All pariking orbits that have an inclination of 28° are plotted. Then a curve fitting algorithm runs a third degree polynomial thru these points (see Figure (9)). Examining the right side of the curve in Figure (9), shows the eccentricity increasing as the semi-major axis increases. The reason for this is that the larger values of eccentricity cause the perigee point to dip deeper into the atmosphere. The increased atmospheric density and the larger velocity of the ET at perigee produces a greater drag

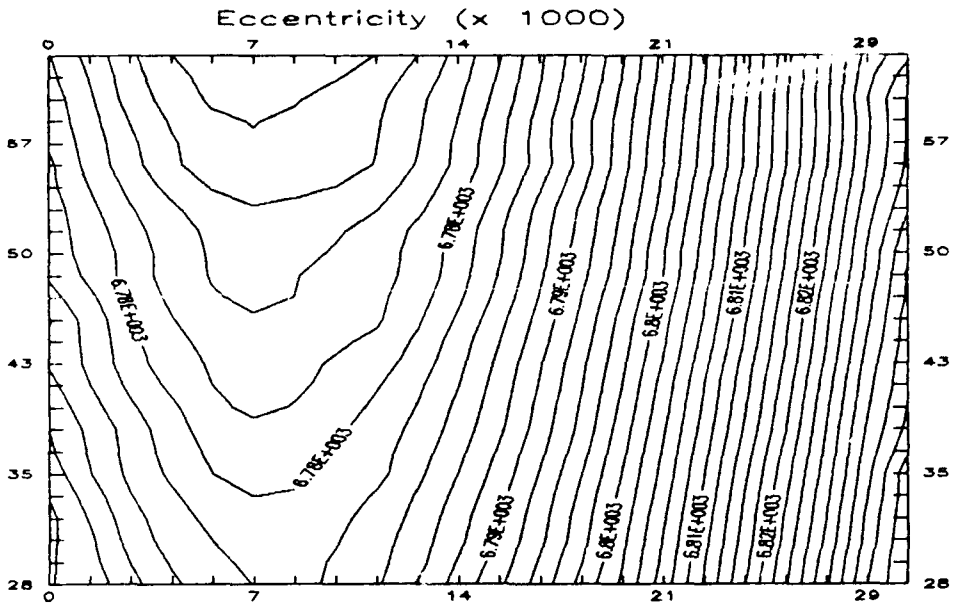

Fig. 10 Contour Map of Parking Orbits

force which accelerates orbital decay. On the left side of the curve, as the eccentricity increases the semi-major axis decreases until it reaches a turning point and then it starts increasing. As the perigee point gets lower (increasing eccentricity) the apogee point increases in altitude. Therefore, at the far left on the curve the increase in apogee altitude (due to increasing eccentricity), and its corresponding decrease in orbital speed and atmospheric density, offsets the increases caused by the lower perigee

altitude. This continues up to the inflection point, and then the increases in density and speed at perigee overcome the apogee effects.

The expression for an orbits energy

$$E = -\frac{\mu}{2a} \tag{67}$$

where E is the specific mechanical energy of a satellite in orbit, shows as the semi-major axis decreases the energy of the orbit also decreases. Therefore, if the ET's orbit has the smallest possible semi-major axis it also minimizes its orbital energy. A low energy orbit costs less to achieve. Therefore, this study concentrated on finding minimum energy parking orbits. Finding the minimum of the curve in Figure (9) was done by taking the derivative of the curve's equation and setting it equal to zero (the equation for this curve and its minimum point are in Appendix C).

To examine the effects of varying inclination on the semi-major axis it is more convenient to look at a topographical map of the data. Figure (10) shows the minimum point for the curve in Figure (9) forms a trough when expanded along the inclination axis. If this trough were

level all of the contour lines would be parallel. However,the contour lines curve inward instead. This indicates the trough is really a "valley", with the "downhill"

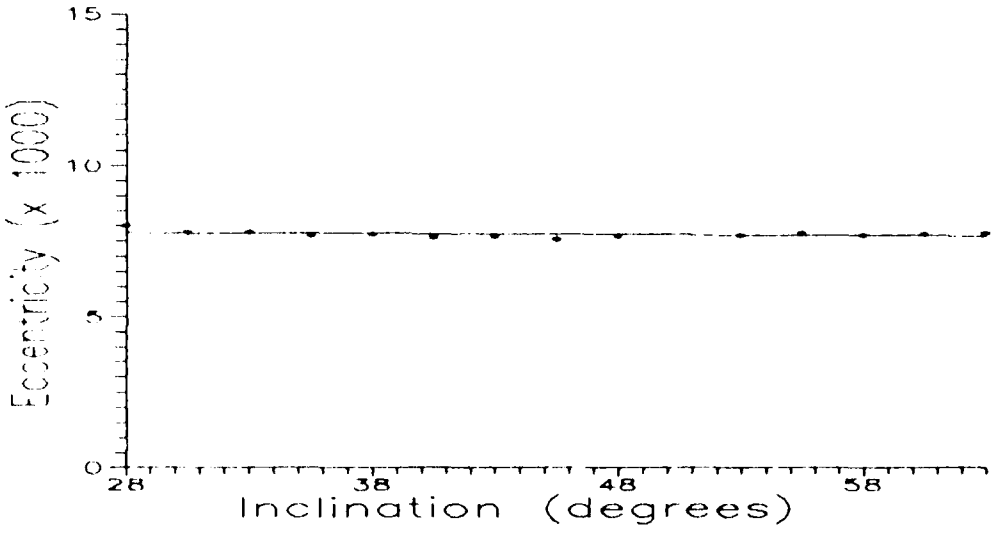

Fig. 11 Inclination and Eccentricity Plane

direction along the axis of increasing inclination. Unfortunately, it is not possible to precisely measure the slope of the valley, or even tell if it is linear from the contour map.

To find the characteristics of the "valley", the surface was cut into cross sections of constant inclina-

tion. Figure (9) was the first of these cross sections. Fourteen more cross sections were made at steps of 2.5° in inclination. As before, the first derivative test is applied to find the minimum points of these curves (Appendix C contains all these equations and minimum points). A curve was then run through these points. In the inclination and eccentricity plane this curve is a straight line of almost constant eccentricity (see Figure (11)). The equation for this line is

$$e_{1000} = 7.8694 - 0.00329834i \qquad (68)$$

where i is the inclination in degrees, and e_{1000} is 1000 times the eccentricity. Because of statistical errors in the curve fitting algorithms (i.e. a "best fit" curve made of points from other "best fit" curves), the slope of this line is small enough to ignore, and eccentricity can be assumed to be constant along the "bottom of the valley".

Next, the inclination and the semi-major axis plane was examined. From the graph of the minimum points, it can be seen that the semi-major axis decreases linearly with increasing inclination (see Figure (12)). The equation for this line is

$$a = 6795.24 - 0.334833i \qquad (69)$$

where a is the semi-major axis in kilometers, and i is the inclination in degrees.

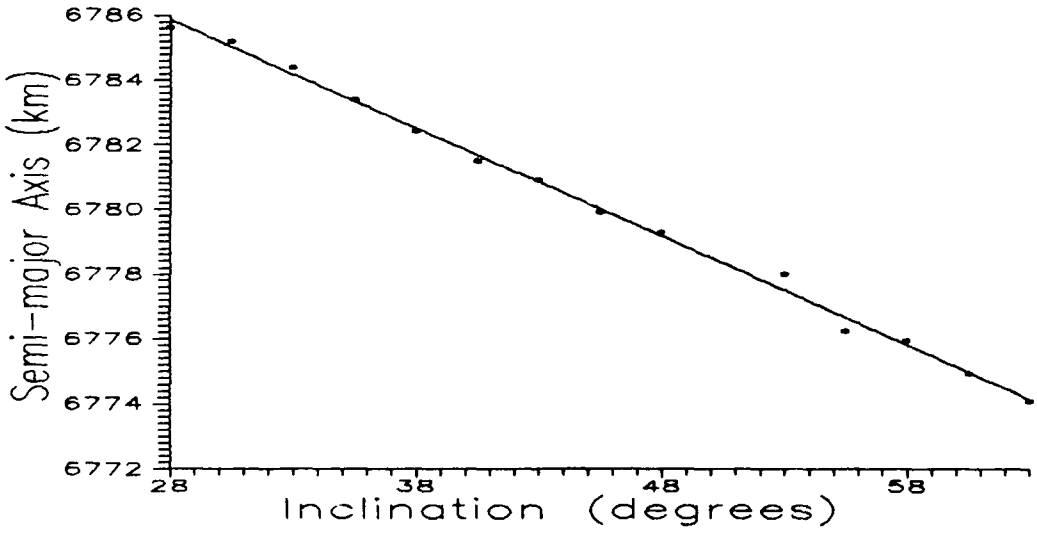

Fig. (12) Inclination and Semi-major Axis Plane

The slope of this line is more than a kilometer decrease in the semi-major axis for every three degree increase in inclination. Therefore, to minimize the semi-major axis the largest possible inclination should be used.

The reason the semi-major decreases with increasing

inclination is due to the Earth's equatorial bulge. Not only does the Earth bulge at the equator, but the atmosphere also bulges. Therefore, when a satellite is over the equator it is experiencing a higher atmospheric density than it would at a higher latitude with the same geocentric altitude. This increase in density causes a linear increase in the drag acting on an external tank. The longer an ET has to stay in this equator bulge (i.e. low inclination orbits) the more energy it requires (larger semi-major axis) to meet the parking orbit criteria.

All initial orbits for this study had the argument of perigee set equal to zero. Therefore the perigee point was over the equator, where the atmospheric bulge is. Additionally, the Earth's equatorial bulge has a perturbing effect on the argument of perigee, causing it to increase linearly with time (see Figure (13)). This moves the perigee point into the higher latitudes where the atmospheric density is lower. For low inclinatio orbits the effects due to the change in the argument of perigee average out over time. However, this is not true near the critical inclination.

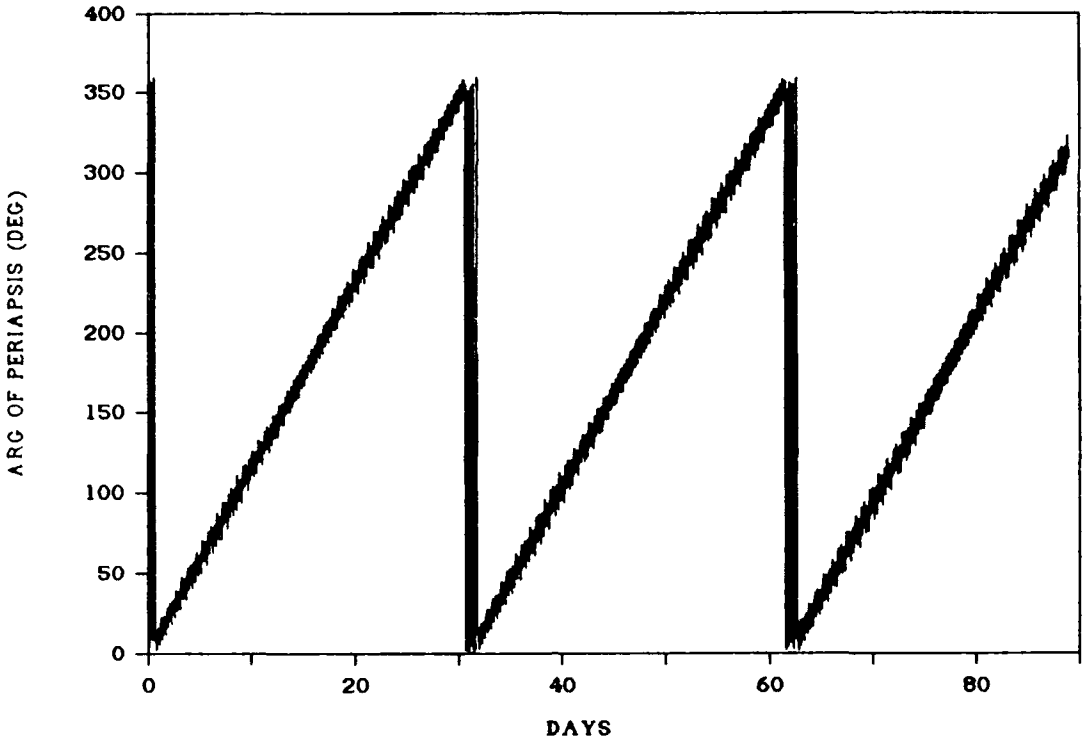

Fig. (13) Linear Variation of ω

At the critical inclination the rate of change of the argument of perigee is zero. This "locks" the perigee point into its initial position. In this study the perigee point would be over the equator, the worst possible location. From the data obtained, the critical inclination does not effect the external tank problem. However, if the argument of perigee could vary instead of being held constant the results would differ.

V CONCLUSION

This study represents the dynamics of an STS external tank in low Earth orbit. A scenario involving an ET parking orbit was developed as a way to limit the scope of the problem. The gravity gradient attitude and the simple atmosphere model were the major assumptions in this investigation.

The major outcome of this study was the determination of a set of initial orbits for the ET which met the parking orbit criteria. In orbital phase space, a surface of these orbits was constructed. An analysis of this surface discovered an optimal parking orbit. In order to minimize orbital energy the semi-major axis must be minimized. This study found that parking orbits with an eccentricity equal to 0.00787 minimized energy and increasing the inclination decreased the semi-major axis. Therefore, the optimal parking orbit would have an eccentricity of 0.00787 and the highest possible inclination (for this study $i_{max} = 63^{o}$).

The optimal eccentricity resulted from the differences of orbital velocity and atmospheric density between apogee and perigee. Higher inclination parking orbits require less energy because the atmosphere bulges at the equator. Extrapolating this concept beyond an inclination of 63^{o}, it may be surmised that the optimal inclination would be 90^{o}.

Here the ET would have the smallest fraction of its orbit in the equatorial bulge. Unfortunately, the Vandenberg, CA launch site will not be used for the STS, thus this orbit is not an option.

This study found the critical inclination did not effect the parking orbits. Since the perigee point was set over the equator, it would remain there for all orbits with a critical inclination. However, if the argument of perigee was set at 90°, then the perigee point would be "locked" into the farthest point from the equatorial bulge. A further study of the critical inclination is recommended. Since this study determined an optimal eccentricity, the eccentricity could be constant and the argue of perigee could vary. The inclination could then range from below to above the critical inclination.

Another area of study could include different methods of changing the external tank's ballistic coefficient (i.e. intentionally tumbling it, thereby reducing its cross-sectional area). Additionally, the results of this study could be used in an analysis of the feasibility of taking the ET into orbit. Questions which could be studied are (1) is the advantage of higher inclinations offset by the decrease of the component of the Earth's rotational velocity in the direction of flight, (2) will placing the ET in a

parking orbit detract from the STS's primary mission, (3) would adding an attitude control system on the ET be worthwhile.

APPENDIX A

Conversion Between Cartesian Coordinates and Orbital Elements

The following algorithm is taken from Reference 19, page 102. Given the six classical elements, a, e, i, Ω, ω, and M, one solves the Kepler's equation to obtain the eccentric anomaly, E, and then computes the following variables:

$$l_1 = \cos(\Omega)\cos(\omega) - \sin(\Omega)\sin(\omega)\cos(i)$$

$$m_1 = \sin(\Omega)\cos(\omega) + \cos(\Omega)\sin(\omega)\cos(i)$$

$$n_1 = \sin(\omega)\sin(i)$$

$$l_2 = -\cos(\Omega)\sin(\omega) - \sin(\Omega)\cos(\omega)\cos(i)$$

$$m_2 = -\sin(\Omega)\sin(\omega) + \cos(\Omega)\cos(\omega)\cos(i)$$

$$n_2 = \cos(\omega)\sin(i)$$

Now the Cartesian coordinates and their associated derivatives can be calculated by solving the following equations:

$$x = a l_1 \cos(E) + b l_2 \sin(E) - a e l_1$$

$$y = a m_1 \cos(E) + b m_2 \sin(E) - a e m_1$$

$$z = a n_1 \cos(E) + b n_2 \sin(E) - a e n_1$$

$$\dot{x} = \frac{na}{r}[b l_2 \cos(E) - a l_1 \sin(E)]$$

$$\dot{y} = \frac{na}{r}[b m_2 \cos(E) - a m_1 \sin(E)]$$

$$\dot{z} = \frac{na}{r}[b n_2 \cos(E) - a n_1 \sin(E)]$$

where $r = \sqrt{x^2 + y^2 + z^2}$

$$n = \sqrt{\mu / a^3}$$

$$b = a\sqrt{1 - e^2}$$

The conversion from Cartesian elements to orbital elements uses the non-singular formulation of Reference 2.

$$a = \left(\frac{2}{r} - \frac{v^2}{\mu}\right)^{-1}$$

$$\bar{e} = -\frac{\bar{r}}{r} - \frac{(\bar{r} \times \bar{v}) \times \bar{v}}{\mu}$$

$$\hat{w} = \frac{\bar{r} \times \bar{v}}{|\bar{r} \times \bar{v}|}$$

$$p = \frac{w_x}{1 + w_z}$$

$$q = \frac{-w_y}{1 + w_z}$$

$$\hat{f} = \frac{1}{1 + p^2 + q^2} \begin{Bmatrix} 1 - p^2 + q^2 \\ 2pq \\ -2p \end{Bmatrix}$$

$$\hat{g} = \frac{1}{1 + p^2 + q^2} \begin{Bmatrix} 2pq \\ 1 + p^2 - q^2 \\ 2q \end{Bmatrix}$$

$$h = \bar{e} \cdot \hat{g}$$

$$k = \bar{e} \cdot \hat{f}$$

$$X_1 = \bar{r} \cdot \hat{f}$$

$$Y_1 = \bar{r} \cdot \hat{g}$$

$$\beta = \frac{1}{1 + \sqrt{1 - h^2 - k^2}}$$

$$\cos(F) = k + \frac{(1 - k^2\beta)X_1 - hk\beta Y_1}{a\sqrt{1 - h^2 - k^2}}$$

$$\sin(F) = h + \frac{(1 - h^2\beta)Y_1 - hk\beta X_1}{a\sqrt{1 - h^2 - k^2}}$$

$$\lambda = F - k\sin(F) + h\cos(F)$$

a, h, k, p, q, and λ are called the equinoctal elements. Their relationship with the classical elements are:

$$a = a$$

$$h = e\sin(\omega + \Omega)$$

$$k = e\cos(\omega + \Omega)$$

$$p = \tan(i/2)\sin(\Omega)$$

$$q = \tan(i/2)\cos(\Omega)$$

$$\lambda = M + \omega + \Omega$$

From the equinoctial elements, any classical elements and related orbital information can be computed.

APPENDIX B

Table of Data Used to Construct Initial Orbit Surfaces

Column #1

e	i	A
32.052	50.5	6848.14
30.980	50.5	6843.14
29.979	50.5	6838.14
28.830	50.5	6833.14
27.680	50.5	6828.14
25.300	50.5	6818.14
22.767	50.5	6808.14
19.785	50.5	6798.14
17.959	50.5	6793.14
30.884	35.5	6848.14
29.811	35.5	6843.14
28.736	35.5	6838.14
27.659	35.5	6833.14
26.435	35.5	6828.14
25.208	35.5	6823.14
23.907	35.5	6818.14
22.677	35.5	6813.14
21.298	35.5	6808.14
19.697	35.5	6803.14
17.946	35.5	6798.14
15.898	35.5	6793.14
13.258	35.5	6788.14
7.371	35.5	6783.14
2.210	35.5	6788.14
29.446	30.5	6843.14
25.995	30.5	6828.14
23.467	30.5	6818.14

Column #2

e	i	A
12.531	45.5	6783.14
26.527	50.5	6823.14
24.071	50.5	6813.14
21.240	50.5	6803.14
0.000	38	6792.14
3.686	43	6783.14
0.000	33	6794.64
0.421	33	6794.00
9.875	33	6785.14
5.748	33	6785.14
18.107	53	6793.14
6.639	53	6778.14
20.726	45.5	6803.14
3.686	45.5	6783.14
14.005	53	6783.14
2.211	53	6783.14
0.000	53	6787.14
0.442	53	6786.14
1.032	53	6785.14
1.621	53	6784.14
15.763	48	6788.14
0.000	48	6788.14
11.284	53	6779.64
2.948	48	6783.14
0.589	48	6787.14
1.179	48	6786.14
6.786	48	6779.14

22.236	30.5	6813.14
20.784	30.5	6808.14
19.109	30.5	6803.14
3.388	30.5	6788.14
1.104	30.5	6793.14
24.640	43	6818.14
23.337	43	6813.14
18.387	38	6798.14
2.210	38	6788.14
31.833	48	6848.14
29.760	48	6838.14
27.460	48	6828.14
25.080	48	6818.14
23.924	48	6813.14
22.547	48	6808.14
17.665	48	6793.14
32.272	53	6848.14
31.126	53	6843.14
28.976	53	6833.14
27.972	53	6828.14
25.520	53	6818.14
22.914	53	6808.14
31.608	53	6803.14
20.005	53	6798.14
16.205	53	6788.14
30.834	48	6843.14
28.684	48	6833.14
26.381	48	6823.14
21.166	48	6803.14
19.564	48	6798.14
0.736	33	6793.14
2.946	33	6788.14

5.457	48	6780.14
4.129	48	6781.14
5.290	53	6779.00
9.144	48	6780.14
7.078	43	6781.14
5.013	43	6782.14
0.000	43	6790.64
8.478	38	6782.14
7.298	38	6782.64
0.000	40.5	6791.14
7.005	40.5	6780 64
8.994	40.5	6782.14
0.000	45.5	6790.14
6.932	45.5	6780.14
4.866	45.5	6781.14
0.000	35.5	6793.14
7.664	30.5	6785.14
0.000	30.5	6795.14
4.716	35.5	6785.14
11.348	35.5	6785.14
32.564	58	6848.14
30.418	58	6838.14
25.813	58	6818.14
24.511	58	6813.14
21.902	58	6803.14
14.742	58	6783.14
32.418	55.5	6848.14
31.418	55.5	6843.14
29.269	55.5	6833.14
28.119	55.5	6828.14
26.967	55.5	6823.14
23.208	55.5	6808.14

16.340	38	6793.14
13.848	38	6788.14
7.518	33	6784.14
31.541	43	6848.14
30.395	43	6843.14
29.248	43	6838.14
28.245	43	6833.14
27.094	43	6828.14
25.941	43	6823.14
22.032	43	6808.14
20.579	43	6803.14
18.829	43	6798.14
16.929	43	6793.14
9.583	38	6783.14
29.665	33	6843.14
17.505	33	6798.14
15.457	33	6793.14
12.669	33	6788.14
19.991	38	6803.14
30.665	33	6848.14
28.517	33	6838.14
27.440	33	6833.14
23.687	33	6818.14
22.457	33	6813.14
19.403	33	6803.14
31.103	38	6848.14
28.955	38	6838.14
27.806	38	6833.14
26.654	38	6828.14
21.518	38	6808.14
30.030	38	6843.14
8.401	28	6785.14

21.755	55.5	6803.14
20.300	55.5	6798.14
20.594	60.5	6798.14
18.695	55.5	6793.14
14.595	55.5	6783.14
6.346	55.5	6776.14
16.868	55.5	6788.14
11.508	55.5	6778.14
9.739	55.5	6777.14
5.755	55.5	6777.14
4.426	55.5	6778.14
0.000	55.5	6786.64
1.474	55.5	6783.14
16.794	58	6788.14
11.803	58	6778.14
10.476	58	6777.14
5.017	58	6777.14
6.346	58	6776.14
4.131	58	6778.14
0.000	58	6785.64
1.327	58	6783.14
25.740	55.5	6818.14
24.511	55.5	6813.14
31.491	58	6843.14
27.114	58	6823.14
30.308	55.5	6838.14
28.229	58	6828.14
23.281	58	6808.14
29.342	58	6833.14
30.418	60.5	6838.14
29.269	60.5	6833.14
28.192	60.5	6828.14

26.215	33	6828.14
24.915	33	6823.14
21.004	33	6808.14
25.501	38	6823.14
24.200	38	6818.14
22.897	38	6813.14
23.320	28	6818.14
11.785	28	6788.14
1.472	28	6793.14
22.016	28	6813.14
20.564	28	6808.14
4.419	28	6788.14
30.300	28	6848.14
28.151	28	6838.14
18.815	28	6803.14
29.226	28	6843.14
24.549	28	6823.14
11.794	43	6783.14
5.160	38	6783.14
13.268	48	6783.14
30.519	30.5	6848.14
28.370	30.5	6838.14
27.220	30.5	6833.14
24.769	30.5	6823.14
17.358	30.5	6798.14
12.227	30.5	6788.14
30.125	53	6838.14
26.674	53	6823.14
31.322	40.5	6848.14
29.101	40.5	6838.14
28.025	40.5	6833.14
26.874	40.5	6828.14

27.040	60.5	6823.14
24.658	60.5	6813.14
23.428	60.5	6808.14
22.049	60.5	6803.14
31.491	60.5	6843.14
18.916	60.5	6793.14
17.162	60.5	6788.14
15.185	60.5	6783.14
6.199	60.5	6775.14
4.870	60.5	6776.14
4.279	60.5	6777.14
12.098	60.5	6778.14
0.000	60.5	6785.14
2.065	60.5	6780.14
3.393	60.5	6778.14
1.179	60.5	6783.14
32.418	63	6848.14
30.418	63	6838.14
28.265	63	6828.14
31.418	63	6843.14
25.960	63	6818.14
27.114	63	6823.14
22.196	63	6803.14
24.732	63	6813.14
23.538	63	6808.14
17.346	63	6788.14
15.480	63	6783.14
19.211	63	6793.14
6.126	63	6774.64
20.741	63	6798.14
4.132	63	6776.14
12.983	63	6778.14

25.721	40.5	6823.14
24.420	40.5	6818.14
23.117	40.5	6813.14
21.739	40.5	6808.14
20.285	40.5	6803.14
18.608	40.5	6798.14
16.634	40.5	6793.14
14.290	40.5	6788.14
10.762	40.5	6783.14
1.473	40.5	6788.14
31.687	45.5	6848.14
30.615	45.5	6843.14
29.540	45.5	6838.14
28.464	45.5	6833.14
27.240	45.5	6828.14
24.860	45.5	6818.14
23.631	45.5	6813.14
22.326	45.5	6808.14
19.196	45.5	6798.14
17.297	45.5	6793.14
15.174	45.5	6788.14

3.541	63	6777.14
11.511	63	6776.14
5.461	63	6775.14
2.950	63	6778.14
12.321	63	6777.14
10.627	63	6775.14
2.508	63	6779.14
1.917	63	6780.14
1.475	63	6781.14
0.000	63	6784.14
1.180	63	6782.14
0.737	63	6783.14
5.600	30.5	6786.14
9.729	35.5	6784.14
5.306	35.5	6784.14
10.315	30.5	6786.14
3.684	35.5	6786.14
3.094	35.5	6787.14
5.750	40.5	6782.14
10.765	45.5	6781.14
11.943	45.5	6782.14

APPENDIX C

Equations for Cross Sections of Constant Inclinations

$I = 28^\circ$

$a = -0.00186798e^{3} + 0.222988e^{2} - 3.02999e + 6797.23$

$I = 30.5^\circ$

$a = -0.00157397e^{3} + 0.194479e^{2} - 2.74247e + 6795.48$

$I = 33^\circ$

$a = -0.00166276e^{3} + 0.198598e^{2} - 2.79726e + 6794.93$

$I = 35.5^\circ$

$a = -0.00150906e^{3} + 0.190148e^{2} - 2.65605e + 6793.28$

$I = 38^\circ$

$a = -0.00157558e^{3} + 0.193635e^{2} - 2.70734e + 6792.48$

$I = 40.5^\circ$

$a = -0.00158724e^{3} + 0.192857e^{2} - 2.66585e + 6791.3$

$I = 43^\circ$

$a = -0.00149035e^{3} + 0.188115e^{2} - 2.61384e + 6790.53$

$I = 45.5^\circ$

$a = -0.00166111e^{3} + 0.198007e^{2} - 2.78083e + 6790.32$

$I = 48^\circ$

$a = -0.00130136e^{3} + 0.179296e^{2} - 2.51682e + 6788.61$

$I = 53^\circ$

$a = -0.00139434e^{3} + 0.183106e^{2} - 2.5692e + 6787.54$

$I = 55.5^\circ$

$a = -0.001721172e^{3} + 0.200656e^{2} - 2.80602e + 6786.73$

$I = 58^\circ$

$a = -0.00168992e^{3} + 0.197474e^{2} - 2.73129e + 6786.02$

$I = 60.5^\circ$

$a = -0.0017882e^{3} + 0.204661e^{2} - 2.83722e + 6785.48$

$\underline{I = 63^{\circ}}$

$a = -0.00177436e^3 + 0.206733e^2 - 2.89023e + 6784.89$

Coordinates for Minimum Points

Inclination	Eccentricity	Semi-major Axis
28	7.9905	6785.61
30.5	7.7879	6785.18
33	7.8082	6784.41
35.5	7.6877	6783.41
38	7.7178	6782.40
40.5	7.6302	6781.48
43	7.6414	6780.88
45.5	7.5577	6779.89
48	7.6569	6779.27
53	7.6913	6777.98
55.5	7.7689	6776.23
58	7.6709	6775.93
60.5	7.7107	6774.95
63	7.7669	6774.08

BIBLIOGRAPHY

1. Born, George H. and Claude E. Hildebrande, Jr. The Conversion of the Spherical Harmonic and Third Body Potential to Keplerian Elements. Contract 9-2619. NASA Manned Spacecraft Center, May 1967.

2. Cook, G.E. "Satellite Drag Coefficients," Planetary and Space Science, 13: 929-946 (October 1965).

3. Covault, Craig "Maui Optical Station Photographs External Tank Reentry, Breakup," Aviation Week and Space Technology, 132: 52-53 (June 1990).

4. Dowd, Douglas L. and B.D. Tapley. "Density Models for the Upper Atmoshere," Celestial Mechanics, 20: 271-295 (October 1979).

5. "External Tank Utilization on Orbit," Space Studies Institute Update, 13: 1-3 (July/August 1987).

6. Fitzpatrick, Philip M. Principles of Celestial Mechanics. New York: Academic Press, Inc. 1970.

7. Gerald, Curtis F. Applied Numerical Analysis (Third Edition). Reading, MA: Addison-Wesling Publishing Company, 1985.

8. Gimarc, Alex J. Report on Space Shuttle External Tank Application. Space Studies Institute, Princeton, NJ, December 1985.

9. Jacchia, Luigi G. "Variations in the Earth's Upper Atmosphere as Revealed by Satellite Drag," Reviews of Modern Physics, 35: 973-991 (October 1963).

10 Jane's Spacefight Directory (Second Edition). London: Jane's, 1986.

11. Jenson, Jorgen and others. Design Guide to Orbital Flight. New York: McGraw-Hill Book Company, 1962.

12 Johnson, Francis S., ed. Satellite Environment Handbook. Stanford, CA: Stanford University Press, 1965.

13 Kane, Thomas R., Peter W. Likiens and David A. Levinson. Spacecraft Dynamics. New York: McGraw-Hill Book Company, 1983.

14. Kaufman, Bernard. "Variation of Parameters and the Long-Term Behavior of Planetary Orbiters." AIAA Paper No. 70-1055, AAS/AIAA Astronautics Conference, 1-3 August 1970.

15. Kaula, William M. Theory of Satellite Geodusy. Waltham, MA: Blaisdell Publishing Company, 1966.

16. King-Hele, Desmond. Theory of Satellite Orbits in an Atmosphere. London: Butterworths, 1964.

17. Kwok, Johnny H. The Artificial Satellite Analysis Program (ASAP). Jet Propulsion Laboratory, 1 April 1985.

18. Martin Marietta Michoud Aerospace. External Tank Gamma Ray Imagining Telescope Study. Contract NAS8-36394, January 1987.

19. Meirovitch, L. and F.B. Wallace, Jr. "On the Effect of Aerodynamic and Gravitational Torques on the Attitude Stability of Satellites," AIAA Journal, 4: 2196-2202 (December 1966).

20. Minor, Maj Dennis D. Orbital Analysis of a STS External Tank in Low Earth Orbit. MS Thesis, AFIT/GA/AA/87D-4. School of Engineering, Air Force Institute of Technology (AU), Wright-Patterson AFB OH, November 1987.

21. National Aeronautics and Space Administration. Spacecraft Aerodynamic Torques. NASA SP-8058. January 1971.

22. National Oceanic and Atmospheric Administration. U.S. Standard Atmosphere, 1976. Washington: NOAA, October 1976.

23. Regan, Frank J. Re-entry Vehicle Dynamics. New York: American Institute of Aeronautics and Astronautics, Inc., 1984.

24. Roy, Archie E. The Foundations of Astronautics. New York: Macmillan, 1965.

25. Sentman, Lee H. and Stanford E. Neice. "Drag coefficients for Tumbling Satellites," Journal o Spacecraft and Rockets, 4: 1270-1272 (September 1967).

26. Silberberg, Rein and others. "Radiation Hadzards in Space," Aerospace America, 25: 38-41 (October 1987).

27. Taff, Laurence G. Celestial Mechanics, A Computational Guide for the Practitioner. New York: John-Wiley and Sons, 1985.

28. Vaughn, Robert L., ed. Space Shuttle, A Triumph in Manufacturing. Dearborn, MI: Society of Manufacturing Engineers, 1985.

29. Vihn, Nguyen X. and others. Hypersonic and Planetary Entry Flight Mechanics. Ann Arbor, MI: The University of Michigan Press, 1980.

30. Wiggins, Lyle E. "Relative Magnitudes of the Space Environmental Torques on a Satellite," AIAA Journal, 2: 770-771 (December 1966).

31. Williams, Richard R. "Drag Coefficients for Astronomical Observatory Satellites," Journal of Spacecraft and Rockets, 12: 74-78 (February 1975).

Vita

Captain James E. Cross was born on 30 April 1958 in Steubenville, Ohio. He graduated from Brooke County High School in Wellsburg, West Virginia in 1976 and attended the U.S. Air Force Academy, graduating with a Bachelor of Science in Astronautical Engineering in May 1980. Immediately after graduation he married Carol Ann Larreau. He then began Undergraduate Flying Training at Vance, AFB Oklahoma. The Cross's first son, Daniel, was born there. Upon graduation, he received his wings and served his first tour of duty at Elmendorf AFB, Alaska flying C-130 transports. Soon after arriving in Alaska the Cross's second son, Robert, was born. After upgrading to aircraft commander he was transferred to Little Rock AFB, Arkansas in September 1985. In 1986 the Cross's third and final son, Matthew, was born. He graduated from instructor pilot school in May 1987. He continued to fly C-130's and work as an Airlift Control Element operations officer until entering the School of Engineering, Air Force Institute of Technology, in May 1989.

REPORT DOCUMENTATION PAGE

Form Approved
OMB No 0704-0188

1. AGENCY USE ONLY (Leave blank)	2. REPORT DATE	3. REPORT TYPE AND DATES COVERED
	November 1990	Master's Thesis

4. TITLE AND SUBTITLE

ANALYSIS OF PARKING ORBITS FOR A STS EXTERNAL TANK IN LOW EARTH ORBIT

5. FUNDING NUMBERS

6. AUTHOR(S)

James E. Cross, Capt, USAF

7. PERFORMING ORGANIZATION NAME(S) AND ADDRESS(ES)

Air Force Institute of Technology, WPAFB OH 45433-6583

8. PERFORMING ORGANIZATION REPORT NUMBER

AFIT/GA/ENY/90D-02

9. SPONSORING/MONITORING AGENCY NAME(S) AND ADDRESS(ES)

10. SPONSORING/MONITORING AGENCY REPORT NUMBER

12a. DISTRIBUTION/AVAILABILITY STATEMENT

Approved for public release; distribution unlimited

12b. DISTRIBUTION CODE

A study was conducted of a single external tank in low Earth orbit. Criteria for a parking orbit are then defined. Various orbits are then selected by varying the semi-major axis, eccentricity, and inclination. The resulting equations of motion for each of the above orbits (including atmospheric drag and a 2x0 gravity model) are numerically integrated over a time span of 90 Earth days. An examination was made of the lowest initial altitudes which allowed the external tank to remain in the orbit window.

Keywords:

14. SUBJECT TERMS

External Tank, Orbital Dynamics, Orbital Decay, ~~Orbits~~ Theses (THI)

15. NUMBER OF PAGES

77

16. PRICE CODE

17. SECURITY CLASSIFICATION OF REPORT	18. SECURITY CLASSIFICATION OF THIS PAGE	19. SECURITY CLASSIFICATION OF ABSTRACT	20. LIMITATION OF ABSTRACT
Unclassified	Unclassified	Unclassified	UL